Independent of Renox, NOX5 Promotes Renal Inflammation and Fibrosis in Diabetes by Activating ROS-sensitive Pathways

Independent of Renox, NOX5 Promotes Renal Inflammation and Fibrosis in Diabetes by Activating ROS-Sensitive Pathways

Jay C. Jha,[1] Aozhi Dai,[1] Jessica Garzarella,[1] Amelia Charlton,[1] Sofia Urner,[2] Jakob A. Østergaard,[1,3] Jun Okabe,[1] Chet E. Holterman,[4] Alison Skene,[5] David A. Power,[6] Elif I. Ekinci,[7] Melinda T. Coughlan,[1] Harald H.H.W. Schmidt,[8] Mark E. Cooper,[1] Rhian M. Touyz,[9] Chris R. Kennedy,[4] and Karin Jandeleit-Dahm[1,2]

Diabetes 2022;71:1282–1298 | https://doi.org/10.2337/db21-1079

Excessive production of renal reactive oxygen species (ROS) plays a major role in diabetic kidney disease (DKD). Here, we provide key findings demonstrating the predominant pathological role of the pro-oxidant enzyme NADPH oxidase 5 (NOX5) in DKD, independent of the previously characterized NOX4 pathway. In patients with diabetes, we found increased expression of renal NOX5 in association with enhanced ROS formation and upregulation of ROS-sensitive factors early growth response 1 (EGR-1), protein kinase C-α (PKC-α), and a key metabolic gene involved in redox balance, thioredoxin-interacting protein (TXNIP). In preclinical models of DKD, overexpression of *NOX5* in *Nox4*-deficient mice enhances kidney damage by increasing albuminuria and augmenting renal fibrosis and inflammation via enhanced ROS formation and the modulation of EGR1, TXNIP, ERK1/2, PKC-α, and PKC-ε. In addition, the only first-in-class NOX inhibitor, GKT137831, appears to be ineffective in the presence of NOX5 expression in diabetes. In vitro, silencing of NOX5 in human mesangial cells attenuated upregulation of EGR1, PKC-α, and TXNIP induced by high glucose levels, as well as markers of inflammation (TLR4 and MCP-1) and fibrosis (CTGF and collagens I and III) via reduction in ROS formation. Collectively, these findings identify NOX5 as a superior target in human DKD compared with other NOX isoforms such as NOX4, which may have been overinterpreted in previous rodent studies.

Diabetes is increasingly recognized as the leading cause of chronic kidney disease. Despite the advent of therapies such as blockade of the renin-angiotensin system and, more recently, sodium–glucose cotransporter 2 (SGLT2) inhibition, a significant number of patients with diabetes still progress to end-stage renal disease requiring costly dialysis and transplantation (1,2). Therefore, there is an urgent need to develop more effective treatments. Enhanced generation of renal reactive oxygen species (ROS), particularly those derived from NADPH oxidases (NOXs), are key mediators of renal inflammation, fibrosis, and mitochondrial dysfunction in diabetic kidney disease (DKD) (3–5). Previous experimental research has focused on the constitutively active NOX isoform NOX4 (*Renox*), shown to be pathogenic in murine models of DKD (4–9). Although NOX4 is deleterious in experimental DKD, it

[1]Department of Diabetes, Central Clinical School, Monash University, Melbourne, Victoria, Australia
[2]Institute for Clinical Diabetology, German Diabetes Centre, Leibniz Centre for Diabetes Research at Heinrich Heine University, Dusseldorf, Germany
[3]Steno Diabetes Centre Aarhus, Aarhus University Hospital, Aarhus, Denmark
[4]Department of Medicine, Kidney Research Centre, Ottawa Hospital Research Institute, Ottawa, Ontario, Canada
[5]Department of Anatomical Pathology, Austin Health, Heidelberg, Victoria, Australia
[6]Department of Nephrology, Austin Health, Heidelberg, Victoria, Australia
[7]Department of Medicine, Austin Health, University of Melbourne, Parkville, Victoria, Australia
[8]Department of Pharmacology and Personalised Medicine, School for Mental Health and Neuroscience, Faculty of Health, Medicine, and Life Sciences, Maastricht University, Maastricht, the Netherlands
[9]Institute of Cardiovascular and Medical Sciences, University of Glasgow, Glasgow, U.K.

Corresponding author: Karin Jandeleit-Dahm, Karin.jandeleit-dahm@monash.edu

Received 2 December 2021 and accepted 27 February 2022

This article contains supplementary material online at https://doi.org/10.2337/figshare.19323524.

provides vasculoprotection in the context of atherosclerosis (10–12), reducing the enthusiasm for NOX4 as a sole target of new treatments in diabetic complications. In addition, the only currently available NOX inhibitor, GKT137831, predominantly blocks renal NOX4 (13), shown to be renoprotective in experimental DKD (5,14), but clinical results indicated this drug was ineffective in treating patients with type 2 diabetes and nephropathy (15).

There is increasing evidence that an alternative isoform, NOX5, which is expressed in humans but not in rodents, plays a crucial role not only in DKD (3,16–18) but also in retinopathy (19), cardiovascular (20,21), and cerebrovascular (22) diseases. Indeed, NOX5 is highly upregulated in association with enhanced ROS formation in kidney biopsy specimens of patients with diabetes (3,17). Recently, it has been demonstrated that *Nox4* wild-type mice with overexpression of human *NOX5* in renal cells, specifically in podocytes and endothelial or smooth muscle cells (SMCs) showed accelerated renal injury in DKD (3,16–18). Both NOX4 and NOX5 are expressed endogenously in humans. It appears that NOX4 is pathogenic in murine models of DKD in the absence of NOX5, whereas NOX5 appears to be relevant in human DKD. However, the role of NOX5, independent of the NOX4 pathway in DKD, has not been determined, because preclinical murine models express *Nox4* but not *Nox5*. Thus, it has been difficult to determine the distinct roles of NOX4 versus NOX5 in DKD. We previously localized the expression of NOX5 in mesangial cells in human kidney biopsy specimens with increased expression in patients with diabetes and nephropathy (17). In the present study, we investigated the role of NOX5 independent of the NOX4 pathway in humanized transgenic (Tg) mice with specific expression of *NOX5* in SMCs, which represent mesangial cells in the kidney in the context of genetic deletion or pharmacological NOX4 inhibition, as well as further defining the status of NOX5 and related molecules in human kidney biopsies and cells.

RESEARCH DESIGN AND METHODS

To examine the detrimental role of NOX5 independent of the NOX4 pathway in DKD, we used genetically modified *NOX5* Tg mice deficient in *Nox4* or NOX4 inhibition by GKT137831 in the presence or absence of diabetes, human mesangial cells silenced for *NOX4* or *NOX5* exposed to high glucose levels, and human kidney biopsy specimens obtained from individuals with and without diabetes. Sample size was chosen based on results of our previous studies (5,17). In general, 15 mice per group were randomly assigned to the respective in vivo study groups. The animal studies were approved by the Alfred Medical Research & Education Precinct Animal Ethics Committee (no. E1493/2014/B; Melbourne, Victoria, Australia) under guidelines laid down by the National Health and Medical Research Council of Australia.

Human Kidney Samples

Human kidney biopsy specimens were obtained from male and female individuals with and without diabetes with nephropathy (estimated glomerular filtration rate, 30–52 mL/min; n = 6/group), and the protocol was approved by the Human Ethics Committee of Austin Health (no. LNR/13/Austin/163; Heidelberg, Victoria, Australia) and complied with the Declaration of Helsinki.

Experimental Animals

NOX5 Tg mice on an FVB/N background with selective expression of the human *NOX5* gene in SMCs, which represent mesangial cells in the kidney, were generated as described previously (3,17,18). Briefly, to generate SMC-specific *NOX5* Tg mice, mice of the SM22-tTA-FVB/N strain (SM22; encoded by *Sm22* promoter, also known as *Tagln*) were crossed with mice of the *NOX5* β FVB/N strain (Clontech, Mountain View, CA) to produce $Sm22^{+}NOX5^{+}$ and $Sm22^{+}NOX5^{-}$ mice. A subgroup of $Sm22^{+}NOX5^{+}$ mice were crossed with in-house–established $Nox4^{-/-}$ mice (5,23) on an FVB/N background to generate $Sm22^{+}NOX5^{+}/Nox4^{-/-}$ and $Sm22^{+}NOX5^{-}/Nox4^{-/-}$ mice.

Diabetes was induced in 6-week-old male $Sm22^{+}NOX5^{+}/Nox4^{-/-}$ and $Sm22^{+}NOX5^{-}/Nox4^{-/-}$ mice by five daily intraperitoneal injections of streptozotocin (STZ; Sigma-Aldrich, St Louis, MO) at a dose of 55 mg/kg in citrate buffer, with control mice receiving citrate buffer alone, and the study was followed for 10 weeks. In parallel to genetic deletion, a pharmacological inhibition of NOX4 by GKT137831 was used. A subgroup of male diabetic and nondiabetic control $Sm22^{+}NOX5^{+}$ and $Sm22^{+}NOX5^{-}$ mice were administered the NOX inhibitor GKT137831 daily by gavage at a dose of 60 mg/kg per day for 10 weeks, commencing with the last injection of STZ.

Mice were placed individually into metabolic cages (Iffa Credo, Lyon, France) for 24 h at week 9 for the collection of urine. Blood glucose, glycated hemoglobin, and systolic blood pressure levels were measured as described previously (5,17). Urinary albumin concentration was measured by using a mouse albumin ELISA quantification kit (Bethyl Laboratories, Montgomery, TX). Urinary and plasma creatinine levels were determined with the Cobas Integra 400 Plus analyzer (Roche Diagnostics, Indianapolis, IN). Creatinine clearance and the urinary albumin to creatinine ratio were determined as previously described (5,17,18). A mouse cystatin C ELISA kit (BioVendor, Brno, Czech Republic) was used to determine plasma cystatin C levels according to the manufacturer's instructions. After 10 weeks (i.e., at 16 weeks of age), mice were anesthetized by intraperitoneal injection of sodium pentobarbital (100 mg/kg body weight; Euthatal; Sigma-Aldrich, Castle Hill, Australia). Only mice with blood glucose $\geq$15 mmol/L were included in the experiments; mice with blood glucose $<$15 mmol/L and with polycystic kidneys were excluded from the study ($<$5% of the total number of mice).

Quantitative RT-PCR In Vivo

Total RNA from the renal cortex of mice was extracted with Trizol and analyzed, and cDNA was generated as described previously (5,17). Gene expression, using mouse probes and primers as described in Supplementary Table 2, was analyzed quantitatively and reported relative to the expression of the housekeeping gene 18S (18S ribosomal RNA Taqman Control Reagent Kit) using the Taqman system (ABI Prism 7500; Perkin-Elmer, Poster City, CA). Results were expressed relative to respective nondiabetic control mice without *NOX5* expression, which were arbitrarily assigned a value of 1.

Renal Histology and Immunohistochemistry

Paraffin-embedded kidney sections, 3 μm thick, were stained with periodic acid-Schiff to assess mesangial area, glomerulosclerotic index (GSI) and tubulointerstitial injury (TII), as described previously (5,17). Immunostaining for glomerular nitrotyrosine (rabbit anti-nitrotyrosine, catalog no. ab5411; Millipore, Billerica, MA), collagen IV (goat anti–type IV collagen, catalog no. 1340–01; Southern Biotech, Birmingham, AL), and CD68 (rabbit polyclonal anti-CD68, catalog no. ab125212; LSBio, Seattle, WA) was performed as described previously (5,17). Sections were then examined under a light microscope (Olympus BX-50; Olympus Optical, Tokyo, Japan) with 20 glomeruli being captured per kidney for the assessment of mesangial area and quantification of nitrotyrosine and collagen IV (percentage of glomerular area) using Image-Pro plus 7.0 software (Media Cybernetics, Bethesda, MD). Additionally, 10 tubulointerstitial fields per kidney were captured for the assessment of TII. GSI and TII were graded, as described previously (5,17). For CD68, the number of positively staining macrophages within each glomerulus was counted. All assessments were performed in a blinded manner. Results were expressed relative to respective nondiabetic control mice without *NOX5* expression, which were arbitrarily assigned a value of 1.

Immunofluorescence

After dewaxing, human kidney biopsy specimens were fixed in 4% paraformaldehyde for 15 min, permeabilized using 0.1% Triton X-100, and incubated in a blocking buffer (1% BSA, 0.25% Triton X in PBS, pH 7.4). Double immunostaining for NOX5 with nitrotyrosine, SM22-α, EGR-1, PKC-α, TXNIP, and NOX4 in human kidney biopsy specimens was performed by incubation with respective primary antibodies to NOX5 (goat polyclonal, catalog no. NBP1–68862; Novus Biologicals, Centennial, CO), nitrotyrosine (rabbit anti-nitrotyrosine, catalog no. ab5411; Millipore), SM22-α (rabbit polyclonal; catalog no. ab14106 Abcam, Cambridge, MA), EGR-1 (rabbit monoclonal, catalog no. 4154S, Cell Signaling Technology, Beverly, MA, USA), PKC-α (rabbit monoclonal, catalog no. ab32376; Abcam), TXNIP (rabbit monoclonal, catalog no. ab188865; Abcam), and NOX4 (rabbit polyclonal, catalog no. ab154244; Abcam) followed by incubation with secondary antibody Alexa Fluor 488 (donkey anti-goat; Invitrogen, Eugene, OR) and Alexa Fluor 568 (donkey anti-rabbit; Invitrogen). All stained sections were examined and images of 3 glomeruli/section of biopsy specimen were taken using a Nikon eclipse-Ni (Tokyo, Japan) fluorescence microscope. Quantitation of glomerular NOX5 fluorescent intensity (percentage of glomerular area) was performed using Image-Pro plus 7.0 software (Media Cybernetics).

Renal MCP-1 ELISA

Protein extracts were obtained from mouse renal cortex for the measurement of renal MCP-1 level, as described previously (5). The Quantikine Mouse MCP-1 ELISA Kit (R&D Systems, Minneapolis, MN) was used to estimate renal and plasma MCP-1 levels, as per the kit instructions. Renal MCP-1 level was expressed relative to total protein concentration.

Western Blot

Renal protein expression by Western blot analysis was performed as described previously (17,18). Briefly, protein extracts from the renal cortex were electrophoresed on 4–20% Mini-PROTEAN precast gels (Bio-Rad Laboratories, Richmond, CA) under nonreducing conditions. Blots were incubated with primary antibodies to the following: EGR-1 (rabbit monoclonal; Cell Signaling Technology), PKC-α (rabbit monoclonal; Abcam) TXNIP (rabbit monoclonal; Abcam), phospho-p44/42 mitogen-activated protein kinase (MAPK; Erk1/2) (rabbit polyclonal, catalog no. 9101; Cell Signaling Technology), and JNK (rabbit polyclonal, catalog no. ab4821; Abcam) overnight at 4°C followed by incubation with goat anti-rabbit secondary antibodies (Dako Corp., Carpinteria, CA). Membranes were subsequently probed for β-actin (Sigma-Aldrich) or α-tubulin (Cell Signaling Technology) to confirm equal loading of samples. Blots were detected using the ECL detection kit (Sigma-Aldrich) and densitometry was performed using Quantity-One software (Bio-Rad Laboratories).

In Vivo Transmission Electron Microscopy

Glomerular basement membrane (GBM) thickness was measured from electron micrographs, as described previously (7,24). Briefly, 1-mm sections of renal cortex were fixed, dehydrated in acetone, and finally embedded in Spurr's resin. Sections were then cut and visualized using a Hitachi 7500 transmission electron microscope (Tokyo, Japan). A total of 8–10 electron micrographs of nonoverlapping fields were taken from each glomerulus at a constant magnification of ×10,000. Thickening of GBM was assessed by measuring the thickness of 12–15 evenly distributed points per capillary loop (7,24), using ImageJ software (National Institutes of Health, Bethesda, MD). An average of 120 points per glomerulus was measured, after which the arithmetic mean ± SEM for GBM thickness was determined for each mouse.

In Vitro Experiments

Human mesangial cells (17) (Clonetics Mesangial Cell Systems; Lonza, Walkersville, MD) were used for in vitro experiments. Human mesangial cells were grown using mesangial cell medium (Lonza) with 10% FCS in a humidified incubator (5% CO_2 at 37°C). The knockdown (KD) of *NOX4* or *NOX5* was performed in human mesangial cells using MISSION shRNA–expressing lentivirus vectors (Sigma-Aldrich), as previously described (17). Cells transduced with the MISSION nontarget shRNA control vector particles (Sigma-Aldrich) were used as controls. The KD efficiency in the cells was verified by RT-PCR and was ~75% for both *NOX4* and *NOX5*. Nontarget and Nox4-shRNA– or Nox5-shRNA–infected cells were then grown in cell media with 5 mmol/L glucose or 25 mmol/L glucose or 5 mmol/L glucose plus 20 mmol/L mannitol and incubated for 24 h at 37°C. Cells were harvested, RNA was extracted by the TRIzol method, and cDNA was synthesized for quantitative RT-PCR, as described previously (5,17). Results were expressed relative to the nontarget control, which was arbitrarily assigned a value of 1. Human probe and primer sequences used for quantitative RT-PCR are listed in Supplementary Table 3.

Measurement of Superoxide In Vitro

Luminol analog L-012 was used to detect superoxide in human mesangial cells. Normal, nontarget, and Nox4-shRNA– or Nox5-shRNA–infected cells were resuspended in 200 mL of RPMI medium at a density of 10^4 cells/well of a 96-well microplate (PerkinElmer) and incubated at 37°C for 24 h. The next day, cells were incubated in a normal glucose concentration (5 mmol/L) or in a high concentration of glucose (25 mmol/L) for 24 h. Each well was washed with Krebs-HEPES, and 100 mL of Krebs-HEPES supplemented with L-012 (100 mmol/L; Wako Chemicals) was subsequently added and incubated at 37°C for 10 min, and plates were read on a luminometer (Berthold Technologies) (5,17). Luminous intensity was measured as relative light units, and results were expressed relative to the nontarget control.

Statistical Analysis

All variables were analyzed by one-way ANOVA using GraphPad Software Prism 7 (San Diego, CA) for multiple comparison of the means followed by Tukey post hoc test or were analyzed by the two-tailed unpaired *t* test when required. $P < 0.05$ was considered statistically significant. Results are expressed as mean ± SEM, unless otherwise specified.

Data and Resource Availability

The data sets used and/or analyzed during this study are available from the corresponding author on reasonable request.

RESULTS

Selection of Preclinical Models

The pathological relevance of NOX4 has been well characterized in murine models of DKD (5,7), but in the absence of *Nox5* expression, because murine models lack the *Nox5* gene. NOX5 is expressed in humans but not in rodents and is reported to be pathogenic in human DKD. However, we have recently demonstrated that in *Nox4* wild-type mice, overexpression of human *NOX5* selectively in SMCs (SMCs represent mesangial cells in the kidney) led to aggravated renal injury in diabetes (17,18). Injury to mesangial cells results in mesangial expansion and glomerulosclerosis, the key features of DKD (4). Thus, to examine the direct causal role of NOX5 in DKD independent of the NOX4 pathway, SMC-specific *NOX5* Tg mice deficient in the *Nox4* gene or treated with the NOX1/4 inhibitor GKT137831 in the absence or presence of STZ-induced diabetes (STZ-diabetes) were used as preclinical models.

Metabolic Variables and Renal Function

To examine the pathogenic role of NOX5 independent of the NOX4 pathway in DKD, SMC ($SM22^+Nox5^+$)-specific *NOX5* Tg mice deficient in *Nox4* or treated with the NOX1/4 inhibitor, GKT137831 in the absence or presence of STZ-diabetes were used as experimental models. All groups of diabetic mice, including $SM22^+Nox5^-/Nox4^{-/-}$ and $SM22^+Nox5^+/Nox4^{-/-}$ mice, as well as $SM22^+Nox5^-$/GKT137831 and $SM22^+Nox5^+$/GKT137831 mice, had elevated levels of plasma glucose and glycated hemoglobin, increased food and water intake, enhanced urine output, as well as reduced body weights and increased kidney weight to body weight ratios, when compared with their respective nondiabetic control groups (Tables 1 and 2). Regardless of *NOX5* expression, no changes in these metabolic variables were observed in the respective control and diabetic mice (Tables 1 and 2). Systolic blood pressure was similar in all groups (Tables 1 and 2). In addition, we examined plasma cystatin C levels and creatinine clearance to assess renal function. All groups of diabetic mice with and without *NOX5* expression had lower levels of plasma cystatin C and increased creatinine clearance than their respective nondiabetic control groups, consistent with hyperfiltration (Tables 1 and 2). *NOX5* expression per se did not alter the state of hyperfiltration.

Upregulation of NOX5 in Association With Enhanced ROS Formation in Human DKD

To examine the clinical relevance of NOX5 versus NOX4 in DKD, immunostaining of human kidney biopsy specimens showed increased expression of glomerular NOX5 (Fig. 1*A* and *B*) in association with enhanced oxidative stress as reflected by enhanced renal intensity of nitrotyrosine in individuals with diabetes compared with those without diabetes (Fig. 1*A*). In addition, a positive correlation between HbA_{1c} and glomerular NOX5 expression was observed in individuals with diabetes (Supplementary Fig. 1 and

Table 1—General and metabolic variables (n = 15/group), plasma cystatin C level, and creatinine clearance (n = 7–10/group) in respective control and diabetic *SM22$^+$Nox5$^-$/Nox4$^{-/-}$* and *SM22$^+$Nox5$^+$/Nox4$^{-/-}$* mice

	SM22$^+$Nox5$^-$/Nox4$^{-/-}$ mice		*SM22$^+$Nox5$^+$/Nox4$^{-/-}$* mice	
	Control	Diabetes	Control	Diabetes
Plasma glucose (mmol/L)	11.0 ± 0.4	33.3 ± 0.1*	11.3 ± 0.5	32.2 ± 0.6†
Glycated hemoglobin (%)	4.1 ± 0.1	11.8 ± 0.3*	4.1 ± 0.1	11.4 ± 0.3†
Glycated hemoglobin (mmol/mol)	21 ± 1.0	105 ± 3.0*	21 ± 1.0	101 ± 3*
Systolic blood pressure (mmHg)	117 ± 5	123 ± 7	118 ± 6	127 ± 8
Food consumption (g)	2.1 ± 0.2	5.6 ± 0.3*	2.4 ± 0.2	5.2 ± 0.4†
Water consumption (mL)	4.1 ± 0.8	23.1 ± 1.3*	3.9 ± 0.7	22.5 ± 1.8†
Urine excretion (mL)	1.1 ± 0.2	19.9 ± 1.2*	0.9 ± 0.2	20.7 ± 1.7†
Body weight (g)	40 ± 1.5	29 ± 1.4*	39 ± 1.5	29 ± 1.1†
Kidney/body weight (mg/g)	5.2 ± 0.1	10.3 ± 0.4*	5.2 ± 0.1	10.2 ± 0.4†
Plasma cystatin C (ng/mL)	431 ± 42	150 ± 15*	492 ± 40	176 ± 29†
Creatinine clearance (mL/min/m^2)	24 ± 4.9	54 ± 12.7*	21 ± 5.4	53 ± 8†

Data are shown as mean ± SEM. *$P < 0.05$ vs. control *SM22$^+$Nox5$^-$/Nox4$^{-/-}$* mice; †$P < 0.05$ vs. control *SM22$^+$Nox5$^+$/Nox4$^{-/-}$* mice.

Supplementary Table 1). The expression level of glomerular NOX4 was not changed in those with diabetes versus those without (Supplementary Fig. 2*A*). Colocalization of NOX5 was observed in human mesangial cells in kidney biopsy specimens (Fig. 1*C*). Therefore, in in vitro experiments using human mesangial cells, we examined the relative expression of NOX isoforms in response to glucose. Like human diabetic kidney biopsy specimens, *NOX5* expression was upregulated ($P < 0.001$) in response to high glucose concentration (Fig. 1*D*), whereas the expression of *NOX4* (Fig. 1*D*) as well as *NOX1* and *NOX2* isoforms remained unchanged (Supplementary Fig. 2*B*).

NOX5 Overexpression Enhances Renal ROS Formation in DKD Independent of NOX4

We examined nitrotyrosine as a marker of ROS, previously shown to be increased by diabetes in the glomeruli of wild-type mice with attenuation in *Nox4* knockout (KO) mice (5,7). In this study, both genetic deletion and pharmacological inhibition of NOX4 by GKT137831 showed no differences in the renal accumulation of nitrotyrosine in diabetic mice compared with their respective nondiabetic control mice (Fig. 1*E–H*). However, diabetic mice with *NOX5* expression in SMCs had an increased accumulation of glomerular nitrotyrosine compared with diabetic animals not expressing NOX5 (Fig. 1*E–H*).

Table 2—General and metabolic variables (n = 15/group), plasma cystatin C level, and creatinine clearance (n = 7–10/group) in respective control and diabetic *SM22$^+$Nox5$^-$*/GKT137831 and *SM22$^+$Nox5$^+$*/GKT137831 mice

	SM22$^+$Nox5$^-$/GKT137831 mice		*SM22$^+$Nox5$^+$*/GKT137831 mice	
	Control	Diabetes	Control	Diabetes
Plasma glucose (mmol/L)	11.9 ± 0.8	32.2 ± 0.8*	11.3 ± 0.7	32.4 ± 0.6†
Glycated hemoglobin (%)	4.1 ± 0.1	9.9 ± 0.2*	4.2 ± 0.1	10.5 ± 0.4†
Glycated hemoglobin (mmol/mol)	21 ± 1.0	85 ± 2.0*	22 ± 2.0	91 ± 4.0†
Systolic blood pressure (mmHg)	105 ± 3	106 ± 2*	105 ± 4	104 ± 3†
Food consumption (g)	4.1 ± 0.2	5.7 ± 0.3*	4.1 ± 0.2	6.1 ± 0.4†
Water consumption (mL)	4.9 ± 0.6	24.1 ± 2.4*	3.9 ± 0.6	26.3 ± 2.3†
Urine excretion (mL)	0.94 ± 0.1	19.3 ± 1.1*	0.78 ± 0.1	21.5 ± 1.6†
Body weight (g)	30 ± 0.7	27 ± 0.5*	30 ± 1.0	27 ± 0.6†
Kidney/body weight (mg/g)	7.2 ± 0.2	10.9 ± 0.4*	7.5 ± 0.1	10.9 ± 0.3†
Plasma cystatin C (ng/mL)	444 ± 49	231 ± 39*	415 ± 25	202 ± 28†
Creatinine clearance (mL/min/m^2)	17 ± 1.7	35 ± 5.1*	12 ± 2.3	30 ± 5.7†

Data are shown as mean ± SEM. *$P < 0.05$ vs. control *SM22$^+$Nox5$^-$*/GKT137831 mice; †$P < 0.05$ vs. control *SM22$^+$Nox5$^+$*/GKT137831 mice.

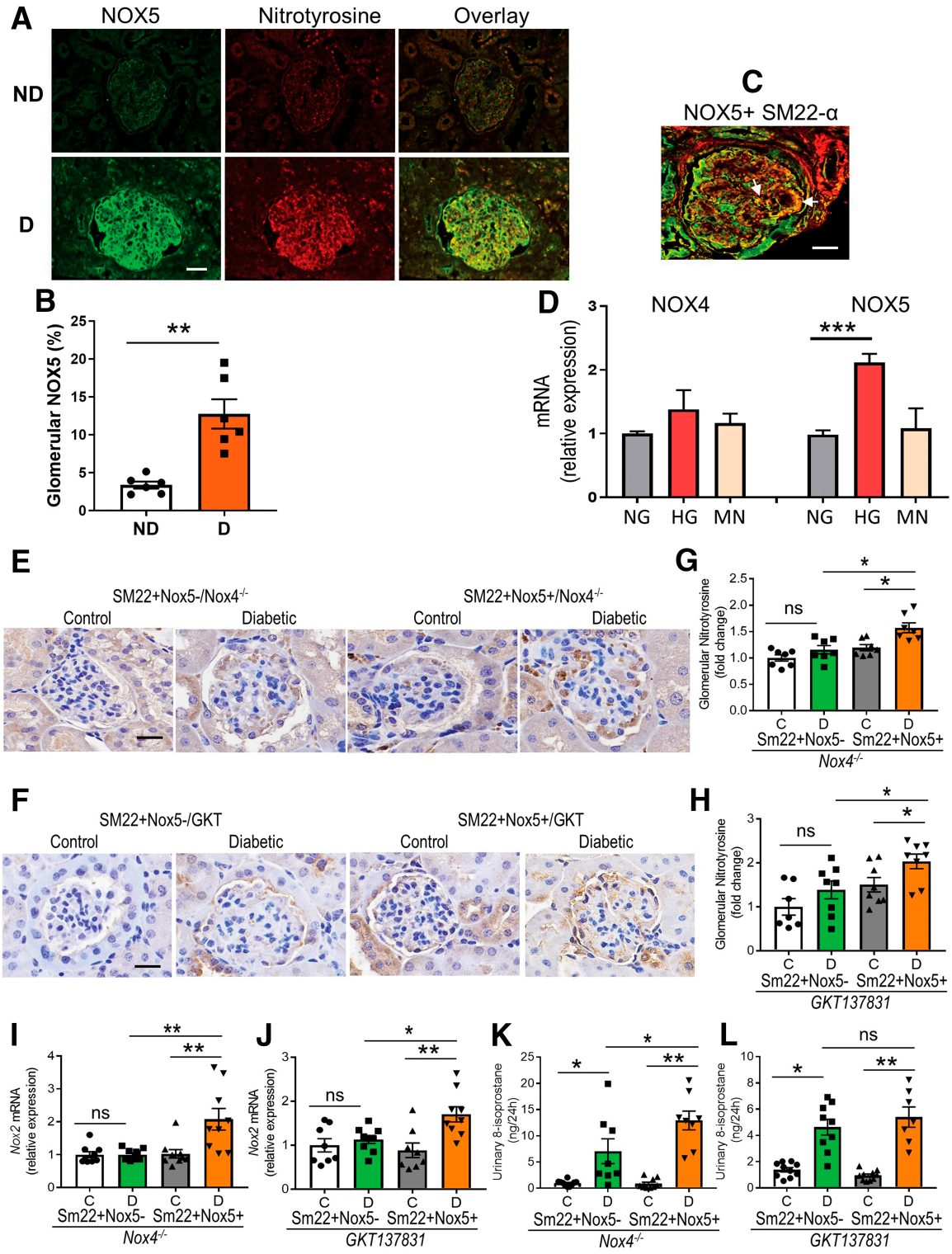

Figure 1—Upregulation of NOX5 in human DKD and overexpression of *NOX5* enhances renal and urinary ROS independent of NOX4 in diabetic mice. *A*: Immunostaining of NOX5 and marker of ROS, nitrotyrosine, and their colocalization in human kidney biopsy specimens obtained from nondiabetic (ND) individuals and patients with diabetes (D). *B*: Quantitation of human glomerular NOX5 in ND and D individuals ($n = 6$ per group). *C*: Colocalization of NOX5 and SM22-α (a marker of SMCs or mesangial cells; yellow staining indicated by arrow) in a human kidney biopsy specimen of patient with diabetes. Scale bar, 50 μm for human kidney biopsy specimens in all photomicrographs. *D*: Gene expression of *NOX4* and *NOX5* in human mesangial cells exposed to normal glucose levels (NG; 5 mmol/L), high glucose levels (HG; 25 mmol/L), and NG plus mannitol (MN; 20 mmol/L; an osmotic control). Immunostaining of nitrotyrosine (*E* and *F*); the quantitation in the glomeruli (*G* and *H*); renal cortical gene expression of *Nox2* (*I* and *J*); and the level of urinary 8-isoprostane (*K* and *L*) in Nox4 knockout (*Nox4*$^{-/-}$) or GKT137831-treated mice with and without *NOX5* expression after 10 weeks of STZ-diabetes. Scale bar, 20 μm in all photomicrographs. Data are shown as mean ± SEM ($n = 7$–10/group). *$P < 0.05$, **$P < 0.01$, ***$P < 0.001$. C, control; D, diabetic; ns, not significant statistically.

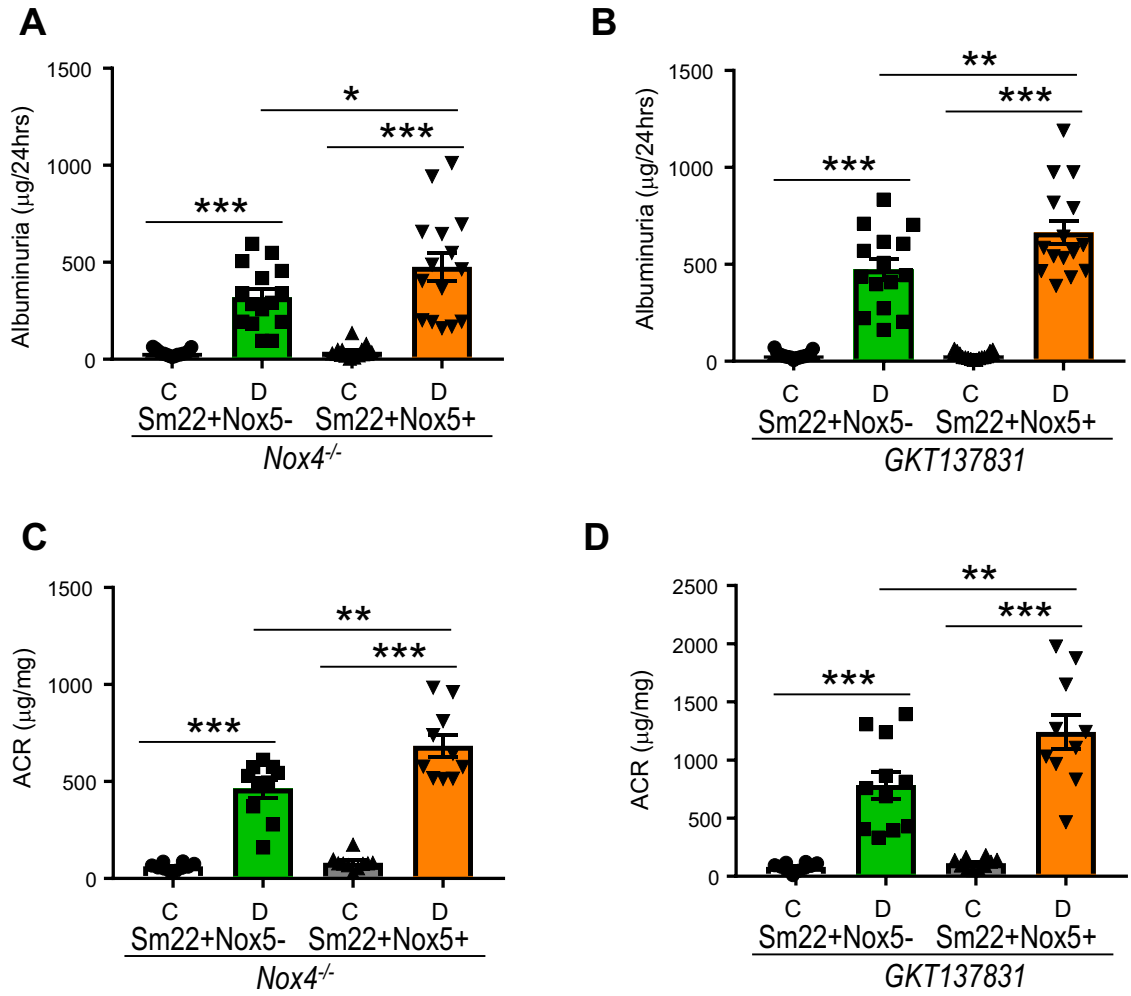

Figure 2—*NOX5* overexpression increases albuminuria in DKD independent of NOX4. Albuminuria (24 h; n = 15/group) (*A* and *B*) and albumin to creatinine ratio (ACR; n = 10/group) (*C* and *D*) in Nox4 KO (*Nox4*$^{-/-}$) mice with and without *NOX5* expression (*A* and *C*) as well as in GKT137831-treated mice with and without *NOX5* expression (*B* and *D*) after 10 weeks of STZ-diabetes. Data are shown as mean ± SEM. *P < 0.05, **P < 0.01, ***P <0.001. C, control; D, diabetic.

Furthermore, we examined the renal expression of *Nox1* and *Nox2* isoforms. *Nox1* expression was almost undetectable. Consistent with glomerular nitrotyrosine, in the absence of *NOX5* expression, renal upregulation of the *Nox2* gene was not seen in diabetic mice with Nox4 deletion or inhibition by GKT137831 (Fig. 1*I–J*). However, in the presence of *NOX5* expression, diabetic mice had upregulation of *Nox2* in the kidney when compared with diabetic mice not expressing *NOX5* (Fig. 1*I–J*). In addition, we examined urinary 8-isoprostane levels as a marker of systemic ROS. Unlike glomerular nitrotyrosine, urinary 8-isoprostane levels remained elevated in diabetic mice despite *Nox4* deletion (Fig. 2*K*) or its inhibition by GKT137831 (Fig. 2*L*). Interestingly, expression of *NOX5* in SMCs led to a further increase in urinary 8-isoprostane levels in *Nox4*-deficient diabetic mice (P < 0.05; Fig. 2*K*).

NOX5 Overexpression Increases Albuminuria in DKD Independent of NOX4

We have previously reported that overexpression of human *NOX5* in Nox4 wild-type mice was associated with accelerated renal injury and albuminuria in diabetes (3,17,18). Therefore, in the present study, we examined the direct causal role of NOX5 in the absence of NOX4. We measured both 24-h urinary albumin excretion (Fig. 2*A* and *B*) and the albumin to creatine ratio (Fig. 2*C* and *D*). Despite genetic deletion or pharmacological inhibition of NOX4, the level of albuminuria was higher (P < 0.001) in all groups of diabetic mice after 10 weeks of diabetes when compared with the respective control groups (Fig. 2*A–D*). Interestingly, there was further significant increase in albuminuria with *NOX5* expression in diabetic mice (Fig. 2*A–D*). *NOX5* expression in SMCs per se did not show any differences in albuminuria in nondiabetic mice (Fig. 2*A–D*).

NOX5 Overexpression Aggravates Glomerulosclerosis in DKD Independent of NOX4

Both mesangial expansion and GSI remained increased in diabetic mice despite *Nox4* deletion or inhibition by

GKT137831, in comparison with their nondiabetic counterparts (Fig. 3*A–F*). In addition, diabetic mice with *NOX5* expression in SMCs had accelerated mesangial expansion and glomerulosclerosis (Fig. 3*A–F*). Furthermore, despite *Nox4* deletion or inhibition, diabetic mice had renal upregulation of the cell proliferation markers *Pcna* and *Ki67* with further upregulation in the presence of *NOX5* expression in SMCs (Fig. 3*G–J*). Moreover, assessment of the glomerular ultrastructure showed increased thickening of the GBM in diabetic mice, which was further increased by *NOX5* expression ($P < 0.05$; Fig. 3*K* and *L*). Unlike GSI, TII remained the same in all respective groups of mice with and without *NOX5* expression in the presence or absence of diabetes (Supplementary Fig. 3*A–D*).

NOX5 Overexpression Exacerbates Renal Fibrosis in DKD Independent of NOX4

In DKD, activation of growth factors is associated with enhanced renal cell proliferation, mesangial expansion, as well as increased extracellular matrix (ECM) accumulation as a result of excessive synthesis of ECM proteins (4). Indeed, consistent with GSI and mesangial expansion, gene expression of classical ECM molecules, including renal *collagen IV* (Fig. 4*A* and *B*) and *fibronectin* (Fig. 4*C* and *D*), *α-SMA* (Fig. 4*E* and *F*), and the growth factor *Ctgf* (Fig. 4*G* and *H*), as well as glomerular deposition of the collagen IV protein (Fig. 4*I* and *L*) remained increased in diabetic mice despite *Nox4* deletion or inhibition by GKT137831. In contrast, all of these ECM molecules and fibrotic markers were further increased by SMC-specific *NOX5* expression and diabetes (Fig. 4*A*−*L*). *NOX5* expression in SMCs, per se, did not appear to result in any differences in the aforementioned fibrotic factors in nondiabetic mice (Fig. 4*A*−*L*).

NOX5 Overexpression Promotes Renal Inflammation in DKD Independent of NOX4

DKD is associated with inflammation, with renal ROS shown to be activating inflammatory cascades (4,25). Similar to the oxidative stress marker nitrotyrosine, a range of proinflammatory markers, including gene expression of renal *Tlr-4* (Fig. 5*A* and *B*), expression of renal *Mcp-1,* both at the gene (Fig. 5*C* and *D*) and protein (Fig. 5*E* and *F*) level, as well as the number of glomerular $CD68^+$ cells (Fig. 5*G* and *H* and Supplementary Fig. 4*A* and *B*) remained unchanged in diabetic mice deficient in *Nox4* or treated with GKT137831, when compared with their respective nondiabetic control mice. In contrast, all of these proinflammatory markers were increased by SMC-specific *NOX5* expression (Fig. 5*A*−*H*). Notably, GKT137831-treated groups of mice with *NOX5* expression had upregulated renal *Tlr-4* even in the absence of diabetes, when compared with control mice not expressing *NOX5* ($P < 0.05$; Fig. 5*B*). Similar to *Tlr-4* and CD68, expression of markers characteristic of M1 macrophages, including *Cd80* and *Tnf-α*, were upregulated in the presence of *NOX5* expression in diabetic mice (Fig. 5*I*−*J*). However, markers characteristic of M2 macrophages such as *Cd204*, *IL-10*, and arginase-1 (*Arg-1*), were not altered by the presence of *NOX5* expression and diabetes in *Nox4* KO mice (Supplementary Fig. 4*C–E*).

Modulation of ROS-Sensitive Factors EGR-1, PKC-α/ε, ERK1/2, and TXNIP by NOX5 in DKD

To further establish the link between NOX5 and important regulatory elements considered relevant to human DKD, we examined the expression of the transcription factor EGR-1; NOX-sensitive PKC-α, a signaling molecule implicated in diabetes associated albuminuria (7,26); and a key metabolic gene involved in redox balance, TXNIP, in the human kidney biopsy specimens as well as in the experimental animals. In humans, we found increased fluorescent intensity of EGR-1, PKC-α, and TXNIP in association with increased *NOX5* expression in the kidneys of individuals with diabetes versus those without (Fig. 6*A*−*C*).

In animals, both renal gene and protein expression of EGR-1 (Fig. 6*D*−*F*), PKC-α (Fig. 6*G*−*I*), and MAPKs, particularly phosphorylated extracellular signal-regulated kinases 1 and 2 (pERK1/2) (Fig. 6*M*−*O*), remained unchanged in *Nox4*-KO diabetic mice without *NOX5* expression compared with the nondiabetic control mice. However, these ROS-sensitive factors were significantly upregulated in the kidney in the presence of *NOX5* expression in the SMCs (Fig. 6*D*−*I* and 6*M*−*O*) of diabetic mice compared with diabetic mice not expressing NOX5. Similar to PKC-α, PKC-ε was upregulated in *NOX5*-expressing diabetic mice (Fig. 6*P*). The expression of renal TXNIP remained elevated ($P < 0.05$) in diabetic mice despite *Nox4* deletion and was further increased with *NOX5* expression ($P < 0.01$) (Fig. 6*J*−*L*). In addition, gene expression of *Egr-1, Pkc-α*, *Txnip, Erk1*, and *Pkc-ε* was increased in nondiabetic mice with *NOX5* expression in comparison with control mice without *NOX5* expression (Fig. 6*D*, *G*, *J*, *M*, and *P*). The protein expression of phosphorylated c-Jun N-terminal kinase (pJNK1) was elevated in both groups of diabetic mice compared with the respective control mice and was not changed in the presence or absence of *NOX5* expression (Fig. 6*Q* and *R*). Similar findings were observed in GKT137831-treated mice with regard to the gene expression of *Egr-1*, *Pkc-α*, and *Txnip* (Supplementary Fig. 5*A–C*), with expression of *NOX5* in SMCs upregulating these key genes. Interestingly, consistent with these ROS-sensitive factors, renal gene expression of *Vegf* was not altered by diabetes alone and was upregulated in the presence of *NOX5* expression and diabetes (Supplementary Fig. 5*D* and *E*).

Silencing of *NOX5* in Human Mesangial Cells Showed Downregulation of ROS-Sensitive Factors *EGR-1*, *PKC-α*, and *TXNIP* and Markers of Inflammation and Fibrosis in DKD

Consistent with the in vivo findings linking NOX5 to proinflammatory, ROS-sensitive factors and profibrotic pathways, in vitro, silencing of *NOX5* in human mesangial cells had a more pronounced attenuating effect on ROS formation induced by high glucose levels (Fig. 7*A*) as well as on downregulation of proinflammatory genes *TLR4*

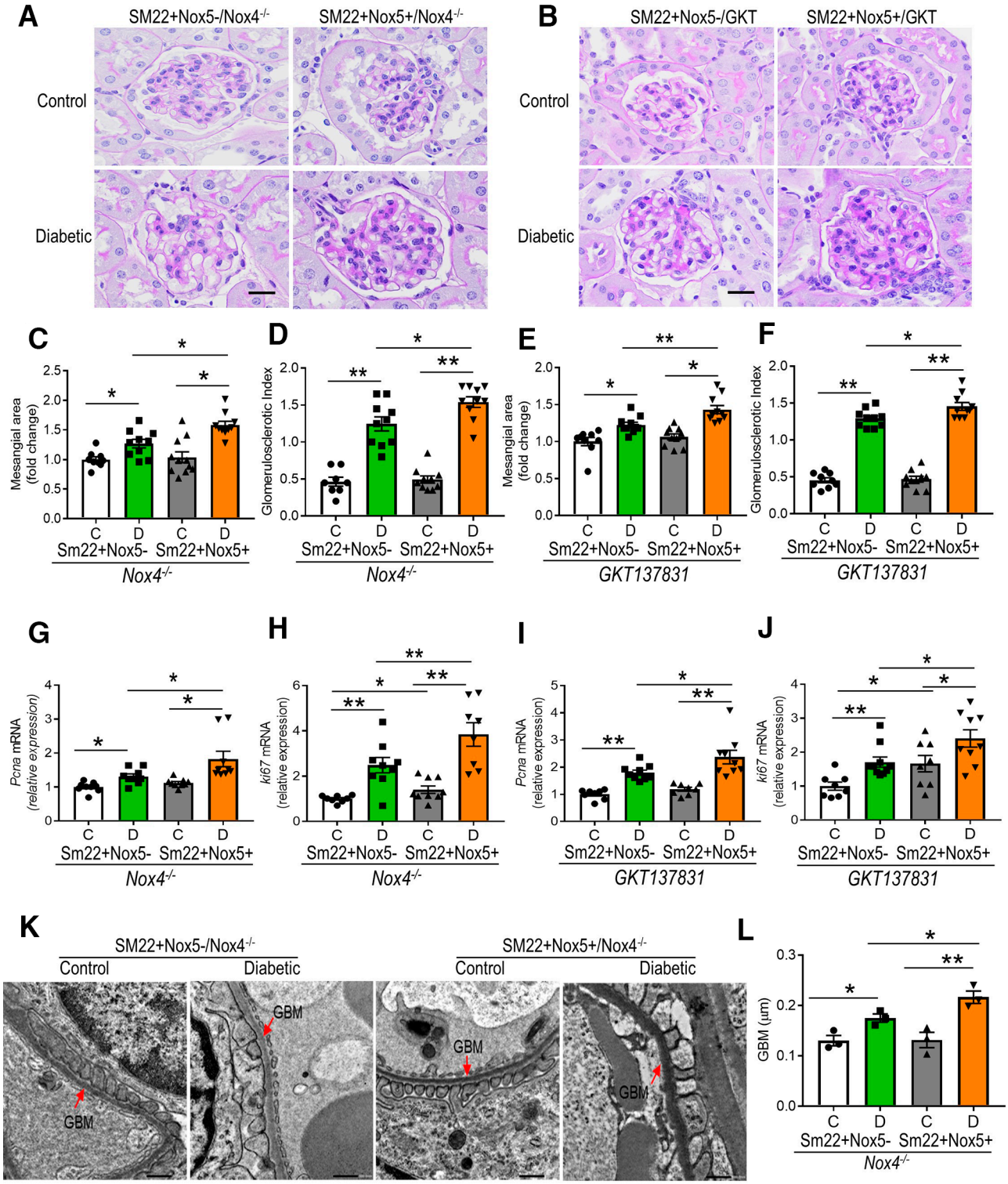

Figure 3—*NOX5* overexpression aggravates glomerulosclerosis and thickening of GBM in DKD independent of NOX4. Periodic acid-Schiff staining (*A* and *B*), relative mesangial area expansion (*C* and *E*), and GSI (*D* and *F*), as well as renal cortical gene expression of *Pcna* (*G* and *I*) and *Ki67* (*H* and *J*) in all groups of Nox4 KO (*Nox4*$^{-/-}$) mice with and without *NOX5* expression or in GKT137831-treated mice with and without *NOX5* expression after 10 weeks of STZ-diabetes. Scale bar, 20 μm in all photomicrographs (n = 8–10/group). *K* and *L*: Transmission electron micrographs showing GBM thickness (n = 3/group; scale bar, 0.5 μm). Data are shown as mean ± SEM. *$P < 0.05$, **$P < 0.01$. C, control; D, diabetic.

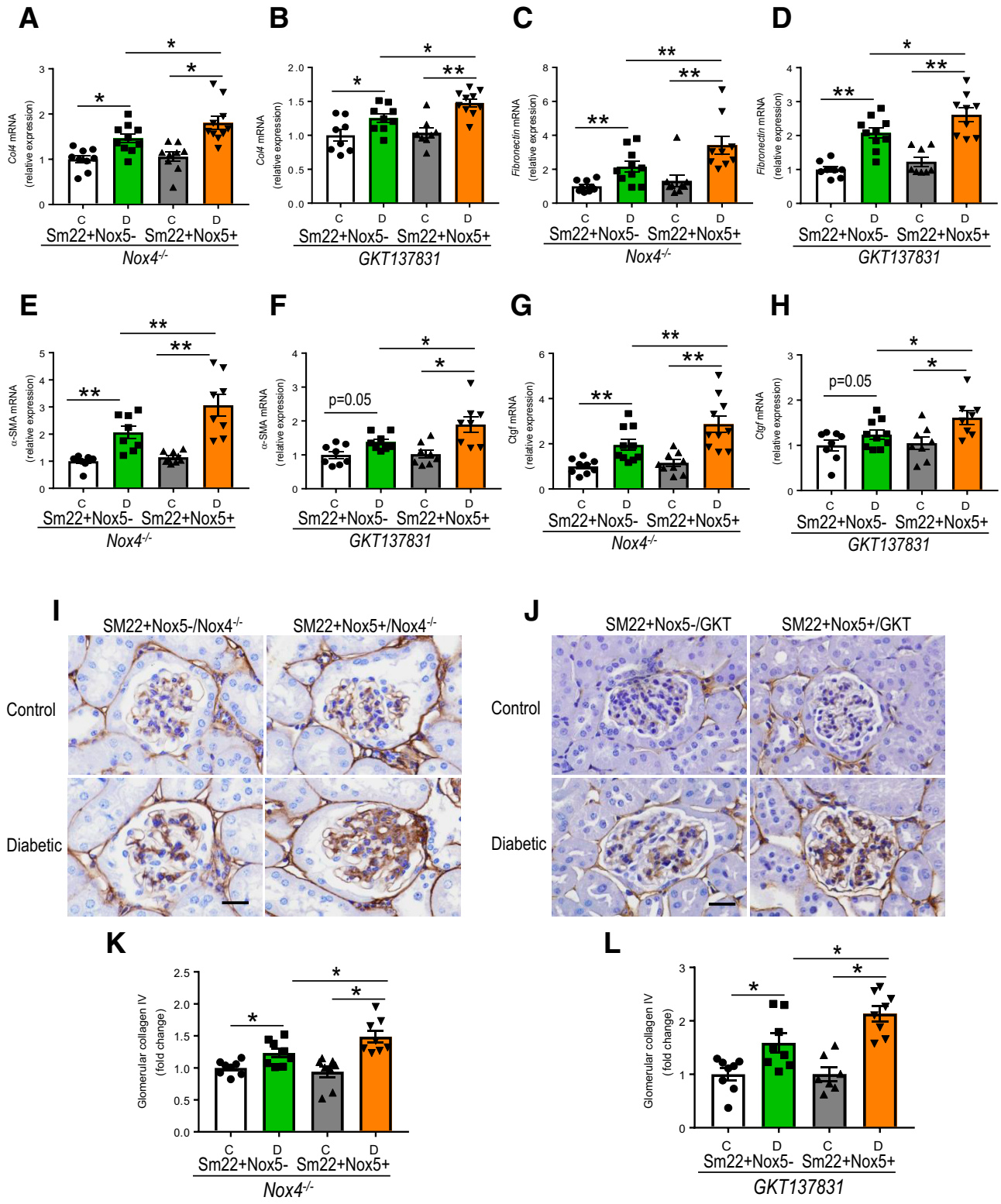

Figure 4—*NOX5* overexpression enhances ECM accumulation and renal fibrosis in diabetes independent of NOX4. Renal cortical gene expression of collagen IV (*A* and *B*), fibronectin (*C* and *D*), α-*SMA* (*E* and *F*), and Ctgf (*G* and *H*), as well as immunostaining of collagen IV (*I* and *J*) and their quantitation (*K* and *L*) in all groups of Nox4 KO (*Nox4*$^{-/-}$) mice with and without *NOX5* expression or in GKT137831-treated mice with and without *NOX5* expression after 10 weeks of STZ-diabetes (n = 8–10/group). Data are shown as mean ± SEM. *$P < 0.05$, **$P < 0.01$. C, control; D, diabetic.

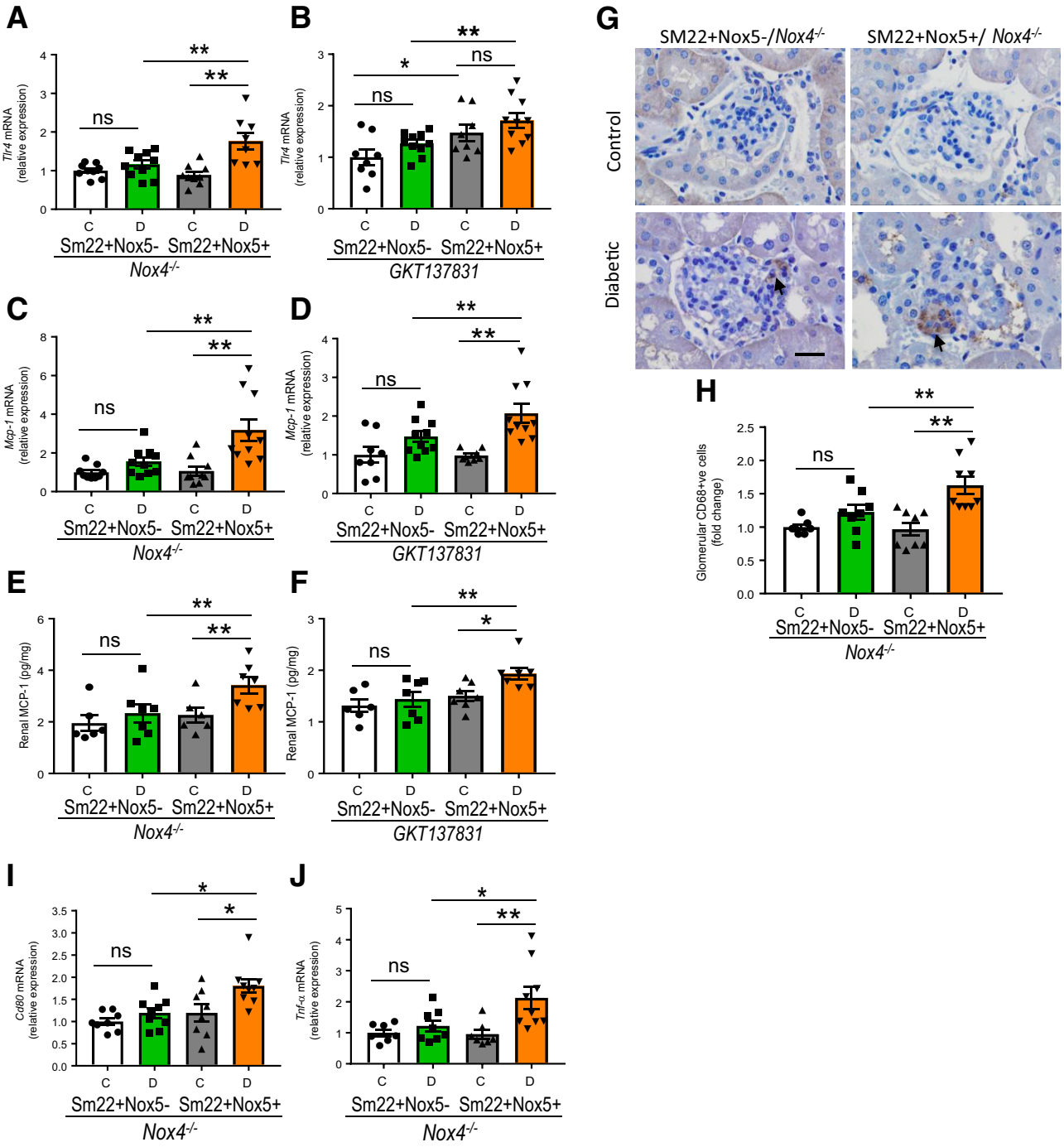

Figure 5—*NOX5* overexpression promotes renal inflammation in DKD independent of NOX4. Renal cortical gene expression of *Tlr-4* (*A* and *B*), *Mcp-1* (*C* and *D*), n = 8–10/group; renal cortical MCP-1 protein levels (n = 6–7/group) (*E* and *F*); in all groups of Nox4 KO (*Nox4*$^{-/-}$) mice with and without *NOX5* expression or in GKT137831-treated mice with and without *NOX5* expression after 10 weeks of STZ-diabetes. Immunostaining of macrophage marker CD68 (*G*) and its quantitation in the glomeruli (*H*)., as well as renal cortical gene expression of *Cd80* (*I*) and *Tnf-α* (*J*) in *Nox4*$^{-/-}$ mice with and without *NOX5* expression after 10 weeks of STZ-diabetes (n = 7–9/group). Scale bar, 20 μm in all photomicrographs. Data are shown as mean ± SEM. *$P < 0.05$, **$P < 0.01$. C, control; D, diabetic; ns, not significant statistically.

and *MCP-1* (Fig. 7*B* and *C*) in comparison with *NOX4* silencing. Furthermore, silencing of *NOX5* showed more robust attenuation of upregulation of ROS-sensitive genes *EGR-1*, *PKC-α*, and *TXNIP* induced by high glucose concentrations when compared with *NOX4* silencing (Fig. 7*D*–*F*). In contrast, silencing of *NOX5*, but not *NOX4*, attenuated upregulation of profibrotic genes including *Ctgf* and *collagen I* and *III* (Fig. 7*G*–*I*) induced by high

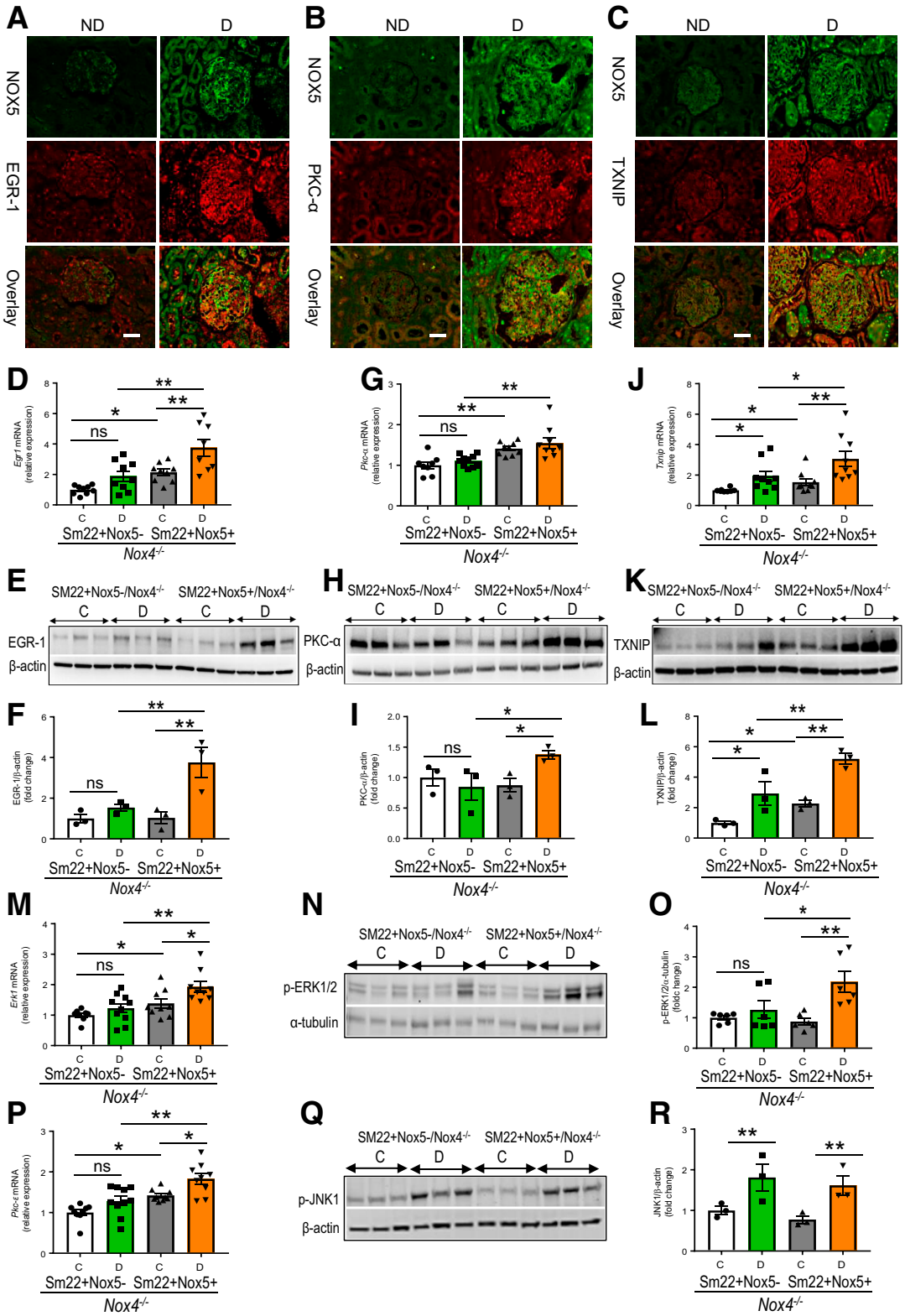

Figure 6—Modulation of ROS-sensitive factors EGR-1, PKC-α/ε, ERK1/2, and TXNIP by NOX5 in DKD. Immunostaining for EGR-1 (*A*), PKC-α (*B*), and TXNIP (*C*) in human kidney biopsy specimens obtained from nondiabetic (ND) individuals and patients with diabetes (D). Scale bar, 50 μm in all photomicrographs. Renal cortical gene (n = 8–10/group) and protein (n = 3–6/group) expression of EGR-1 (*D–F*), PKC-α (*G–I*), TXNIP (*J–L*), and pERK1/2 (*M–O*), as well as gene expression of PKC-ε (*P*) and protein expression of pJNK1 (*Q* and *R*) in all groups of Nox4 KO (*Nox4*$^{-/-}$) mice with and without *NOX5* expression after 10 weeks of STZ-diabetes. Molecular weight of EGR-1 (75 kDa), PKC-α (77 kDa), TXNIP (50 kDa), pERK1/2 (44 and 42 KDa), pJNK1 (49 kDa), β-actin (42 kDa), and α-tubulin (50 kDa). β-actin and α-tubulin are housekeeping proteins. Data are shown as mean ± SEM. *$P < 0.05$, **$P < 0.01$. C, control; D, diabetic; ns, not significant statistically.

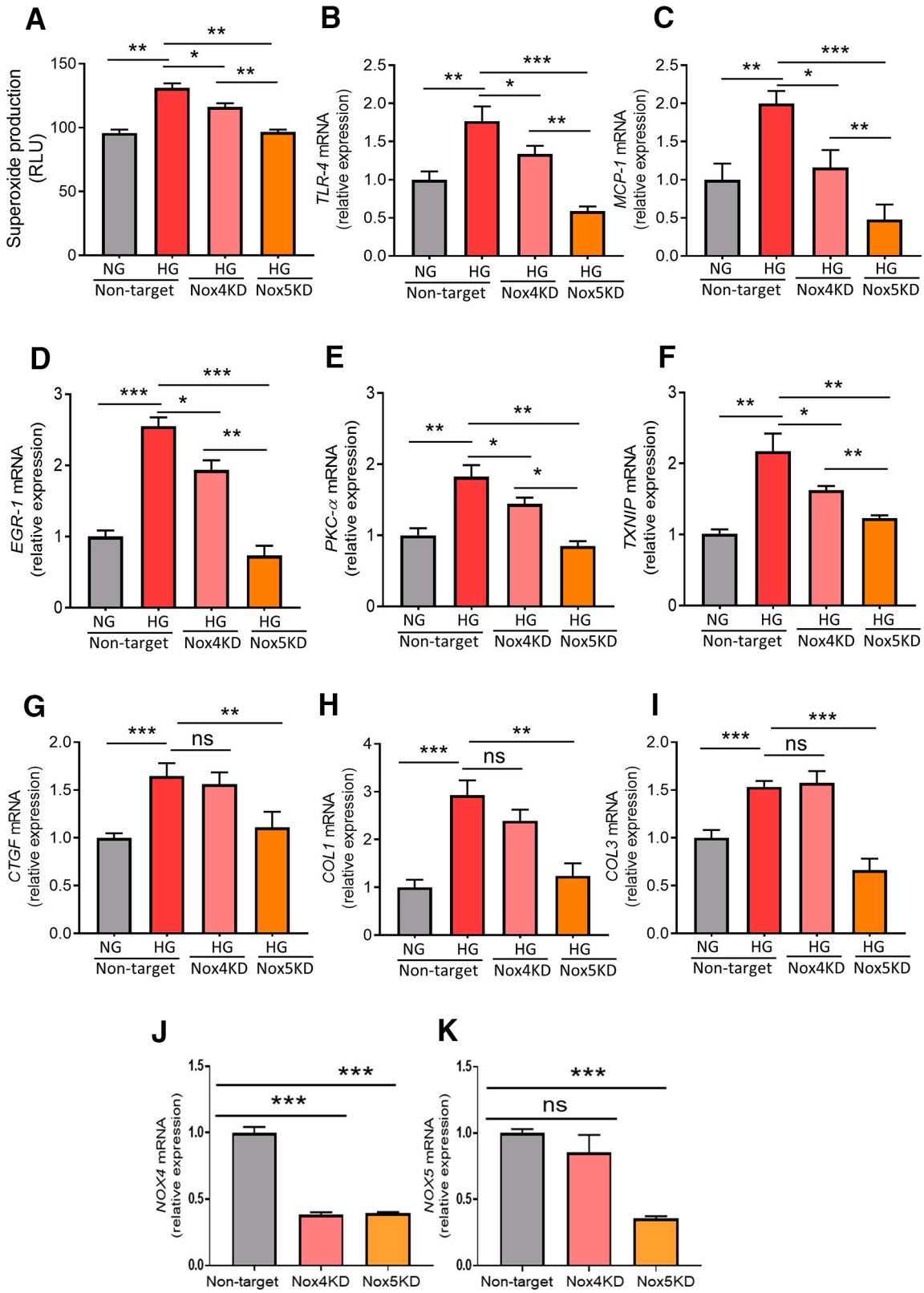

Figure 7—Effect of *NOX4* or *NOX5* silencing on ROS-sensitive factors as well as on markers of inflammation and fibrosis in human mesangial cells exposed to glucose. *A–C*: Relative changes in the level of superoxide production (*A*) and gene expression of markers of inflammation *TLR-4* (*B*) and *MCP-1* (*C*). *D–F*: Gene expression of ROS-sensitive factors *EGR-1* (*D*), *PKC-α* (*E*), and *TXNIP* (*F*). *G–I*: Gene expression of markers of fibrosis *CTGF* (*G*), *collagen I (COL1)* (*H*), and collagen III (COL3) (*I*) in human mesangial cells silenced for *NOX4* (*NOX4* KD) or *NOX5* (*NOX5* KD) in response to normal glucose (NG; 5 mmol/L) and high glucose (HG; 25 mmol/L) levels. *J* and *K*: Gene expression of *NOX4* (*J*) and *NOX5* (*K*) in human mesangial cells with either KD for *NOX4* or *NOX5*, respectively. Data are shown as mean ± SEM. $*P < 0.05$, $**P < 0.01$, $***P < 0.001$. ns, not significant statistically; RLU, relative light unit.

glucose levels, consistent with the dominant role of the pro-oxidant enzyme NOX5 versus NOX4 on renal fibrosis in the context of human DKD. Moreover, we observed that silencing of *NOX5* in mesangial cells showed downregulation of *NOX4* but not vice versa (Fig. 7*J* and *K*).

DISCUSSION

Intrarenal oxidative stress plays a central role in the pathogenesis of DKD (4,27); results of studies of rodents suggest that the NOX family of enzymes, particularly the NOX4 isoform, is a prominent source of renal ROS in both physiological and pathological conditions such as DKD (4,5,7–9). The NOX5 isoform, present in humans but absent from the genome of rodents, increasingly has become recognized for its role in DKD and other diabetic complications (3,16–18). To our knowledge, this is the first comprehensive study in which the pro-oxidant enzyme NOX5 has been identified as a key contributor to DKD, independent of the NOX4 pathway. We demonstrated colocalization of *NOX5* in mesangial cells, with increased expression of NOX5 in kidney biopsy specimens of individuals with diabetes, in association with enhanced ROS formation and NOX5-dependent, ROS-sensitive pathways, including EGR-1, PKC-α, and TXNIP. Furthermore, in human renal cells, we identified upregulation of *NOX5* in response to high glucose concentration and found that silencing of *NOX5* exhibited pronounced attenuation of markers of inflammation, fibrosis, and ROS-sensitive factors via a reduction in ROS formation. Moreover, it appears that *NOX4* is downstream of and potentially regulated by *NOX5*.

In the in vivo setting, we evaluated the pathogenic role of NOX5 independent of the NOX4 pathway. We previously demonstrated that the renoprotective effects of genetic *Nox4* deletion were also conferred by administration of the specific NOX1/NOX4 inhibitor GKT137831 in murine models of DKD (5,14). However, these rodent models do not express *NOX5* naturally (28), and GKT137831 was shown to have, at best, a very weak inhibitory effect on NOX5 (13). Thus, in parallel to genetic deletion of *Nox4*, we examined the effect of this inhibitor, GKT137831, in our *NOX5* Tg mouse models.

NOX5 primarily generates superoxide, which interacts with nitric oxide to form peroxynitrite, in turn resulting in nitrotyrosine formation. Consistent with our previous observations (5,8,14), genetic deletion or pharmacological inhibition of NOX4 did not appear to result in increased ROS formation, as evidenced by a lack of glomerular nitrotyrosine accumulation in diabetic mice. However, *NOX5* expression resulted in enhanced glomerular accumulation of nitrotyrosine in the presence of diabetes. This suggests that NOX4 blockade is insufficient to halt ROS generation in the context of *NOX5* expression, pinpointing NOX5 as the likely source of this increase in intrarenal ROS. This finding confirms and extends in vitro research suggesting that GKT137831 has no major inhibitory effect on NOX5 (13), thereby suggesting that this drug is not sufficiently effective in blocking NOX5-derived ROS in vivo.

There is a bidirectional interplay between renal ROS and inflammation, thereby perpetuating renal injury in DKD (4). TLR4 and the chemokine MCP-1 are modulated by ROS, leading to macrophage infiltration and inflammation in chronic diseases such as DKD (16,18,29–31). Indeed, TLR4 has also been linked to both NOX4 (32,33) and NOX5 (18) in DKD and nondiabetic inflammatory models (16). In the present study, both genetic deletion and pharmacological inhibition of NOX4 in diabetic mice mitigated renal expression of *Tlr4* and *Mcp-1* as well as glomerular $CD68^+$ macrophage deposition and markers characteristic of M1 macrophages, including *Cd80* and *Tnf-α*. Conversely, despite *Nox4* deficiency, *NOX5* expression in diabetic mice enhanced these proinflammatory cascades. Thus, independent of NOX4, NOX5 appears to enhance renal macrophage infiltration and inflammation in DKD. Furthermore, silencing of *NOX5* in human renal cells showed a pronounced attenuation of increased expression of *TLR-4* and *MCP-1* induced by high glucose concentrations. NOX4 blockade completely abrogated mRNA levels of the phagocytic NOX isoform *Nox2* in diabetic mice in the absence of *NOX5*. By contrast, *Nox2* was upregulated in the presence of diabetes and *NOX5*. This observation indicates there is a feedback mechanism activated by NOX5-derived enhanced ROS that augments inflammation in DKD.

To link NOX5-derived, ROS-mediated renal inflammation and fibrosis in DKD, we examined key signaling pathways, including the transcription factor EGR-1; protein kinases PKC-α, PKC-ε, and MAPK (ERK1/2); and the metabolically sensitive gene TXNIP, and their modulation by *NOX5*. EGR-1 is linked to renal inflammation and fibrosis, with *Egr-1*–deficient mice exhibiting improved renal function and reduced structural injury (34). EGR-1 has also been reported to be a potential transcription activator of NOX4 in DKD (34–36). The involvement of PKC-α in albuminuria development in DKD was modulated by both NOX4 and NOX5 (7,9,17,18). Similar to PKC-α, an association between oxidative stress and increased expression of renal PKC-ε has also been reported in a rat model of DKD (37). In addition, activation of the MAPK pathway including ERK1/2 is widely reported in DKD (38).

In our study, genetic deletion or pharmacological inhibition of NOX4 attenuated the increase in renal *Egr-1*, *Pkc-α*, *Pkc-ε*, and *Erk1* expression seen in diabetic mice. However, upregulation of *Egr-1*, *Pkc-α*, *Pkc-ε*, and *Erk1* occurred in the presence of *NOX5* expression, suggesting a direct role for NOX5 in modulating their expression in DKD. Consistent with these findings, *NOX5* KD in human renal cells led to downregulation of *EGR-1* and *PKC-α* in response to high glucose concentration. The metabolic gene *TXNIP* increases ROS by binding and attenuating the antioxidant action of thioredoxin (39–41) in DKD. Increased renal TXNIP has been reported in human

diabetic kidneys (39), whereas *Txnip*-deficient diabetic mice had reduced albuminuria and renal fibrosis via decreased ROS and *Nox4* expression (41). Interestingly, despite *Nox4* deletion, *Txnip* was upregulated in *NOX5*-expressing mice, in the presence or absence of diabetes, suggesting a direct role for NOX5 in regulating TXNIP in DKD. Indeed, our study findings indicate that both NOX4 and NOX5 regulate these key factors and that blockade of NOX4 alone cannot attenuate these molecules in the presence of *NOX5* expression. This is clearly relevant in a human context where both NOX4 and NOX5 are expressed endogenously.

In DKD, renal ROS increase cellular proliferation and differentiation via modulation of genes, including the cell-proliferation markers *Ki-67* and *PCNA* (4,42). Moreover, the growth factor CTGF enhances cell migration, proliferation, and ECM remodeling in DKD (43,44). In addition, activation of both CTGF (45) and α-SMA (46) in the kidney induces epithelial to mesenchymal transition, a process that may contribute to renal fibrosis, including in DKD (47). In this study, despite *Nox4* deletion or inhibition, expression of *NOX5* enhanced the renal upregulation of *Ki67, Pcna, Ctgf*, and *α-SMA* in diabetic mice, suggesting a key role for NOX5 in both renal cell proliferation and fibrosis. Furthermore, independent of NOX4, diabetic mice expressing *NOX5* had more pronounced renal structural injury, with a further increase in mesangial area, glomerular collagen IV deposition, and enhanced glomerulosclerosis than what we observed in diabetic mice without the NOX5 isoform. These overt structural findings seen in *NOX5*-expressing diabetic mice occurred as a result of increased expression of genes implicated in fibrosis, including *collagen IV* and *fibronectin*. Moreover, silencing of *NOX5*, but not *NOX4*, attenuated upregulation of profibrotic genes induced by high glucose concentrations, including *Ctgf* and *Collagen I* and *III*, consistent with the dominant role of the pro-oxidant enzyme NOX5 versus NOX4 in the context of human DKD.

Previously, we demonstrated that blockade of NOX4 attenuated albuminuria in diabetic mice (5,7). In addition, Tg mice expressing *NOX5* in podocytes (3), SMCs (17,18), and endothelial cells (18) led to enhanced albuminuria in diabetes. In this study, despite *Nox4* deletion or pharmacological inhibition, albuminuria remained elevated in diabetic mice, with *NOX5* expression further exacerbating albuminuria in diabetes. Because NOX4 blockade failed to reduce albuminuria in the presence of *NOX5*, these findings emphasize the importance of NOX5 over NOX4, which is a particularly relevant finding in regard to human DKD with expression of both these isoforms. In DKD, renal vascular endothelial growth factor (VEGF) is positively correlated with albuminuria and endothelial dysfunction (48,49). We previously demonstrated a link between NOX4 and VEGF in DKD (5,7). Recently, we also found an association between NOX5 and VEGF, albeit in diabetic retinopathy (19). In this current study, *NOX5* expression modulated *Vegf e*xpression in the kidney independently of NOX4. In addition, correlations between PKC-α activation and VEGF expression, along with albuminuria, have also been reported in DKD in studies in which diabetic *Pkc-α* KO mice had reduced albuminuria and less renal VEGF expression (50,51). It appears that NOX5 is directly involved in modulating both PKC-α and VEGF expression, which perhaps explains the association between NOX5 and enhanced albuminuria in our models. An association between NOX4 and thickening of the GBM, a classical ultrastructural abnormality in DKD (52), has been demonstrated with attenuation of GBM thickening in podocyte-specific *Nox4*-deficient diabetic mice (7). Furthermore, Holterman et al. (3) showed increased GBM thickening in podocyte-specific *NOX5* Tg mice with diabetes. Importantly, independent of NOX4, we found a significant increase in GBM thickness in *NOX5*-expressing diabetic mice.

In conclusion, independent of the NOX4 pathway, the progression of DKD, as evidenced by enhanced renal ROS, inflammation, elevated glomerulosclerosis, and albuminuria in association with ROS-sensitive key factors, EGR1, MAPK (ERK1/2), PKC-α/ε and TXNIP, is accelerated in the presence of *NOX5* expression (Supplementary Fig. 6). Hence, in this study, we provide key evidence for a predominant role for NOX5 in DKD. In addition, we highlight that the only clinically evaluated NOX inhibitor, GKT137831, did not effectively inhibit NOX5-mediated renal injury in DKD. Thus, we clearly demonstrate the predominant role of NOX5 as a prooxidant enzyme in human DKD and provide the impetus for the development of an NOX5-specific inhibitor to alleviate the increasing burden of DKD.

Acknowledgments. The authors thank Professor George Jerums (Department of Endocrinology, Austin Health, University of Melbourne) and Professor Richard J. MacIsaac (Departments of Endocrinology and Diabetes, St Vincent's Hospital and University of Melbourne, Australia) for helping us obtain human kidney biopsy specimens; and E. Lastavec and M. Lyttle (Department of Diabetes, Central Clinical School, Monash University) for experimental animal handling and technical support.

Funding. This work was supported by National Health and Medical Research Council of Australia (NHMRC) project grant APP100585 as well as by Juvenile Diabetes Research Foundation (JDRF) grant 2-SRA 2014-259-Q-R. K.J.-D. and M.E.C. received Senior Research Fellowships from the Australian NHMRC (grants APP1059124 and APP1078808), and J.C.J. received Early Career Research Fellowships from Australian NHMRC (APP1126169) and JDRF (201302918). Genkyotex provided the NOX1/4 inhibitor GKT137831.

Duality of Interest. No potential conflicts of interest relevant to this article were reported.

Author Contributions. J.C.J. and K.J.-D. conceived and designed the research. J.C.J., A.D., J.G., A.C., S.U., J.A.Ø., J.O., and C.E.H. performed the experiments and analyzed the data. A.S., D.A.P., E.I.E., and M.T.C. collected human kidney biopsy samples and gave scientific input. J.C.J. and K.J.-D. wrote and reviewed the manuscript. H.H.H.W.S., M.E.C., R.M.T., and C.R.K provided intellectual input and reviewed the manuscript. J.C.J. and K.J.-D. are the guarantors of this work and, as such, had full access to all of the data in the study and take responsibility for the integrity of the data and the accuracy of the data analysis.

Prior Presentation. This study was presented in oral form at the 56th European Association for the Study of Diabetes Annual Meeting 2020 (virtual), Vienna, Austria, 21–25 September 2020.

References

1. Fioretto P, Zambon A, Rossato M, Busetto L, Vettor R. SGLT2 inhibitors and the diabetic kidney. Diabetes Care 2016;39(Suppl. 2):S165–S171
2. Perkovic V, Jardine MJ, Neal B, et al.; CREDENCE Trial Investigators. Canagliflozin and renal outcomes in type 2 diabetes and nephropathy. N Engl J Med 2019;380:2295–2306
3. Holterman CE, Thibodeau JF, Towaij C, et al. Nephropathy and elevated BP in mice with podocyte-specific NADPH oxidase 5 expression. J Am Soc Nephrol 2014;25:784–797
4. Jha JC, Banal C, Chow BS, Cooper ME, Jandeleit-Dahm K. Diabetes and kidney disease: role of oxidative stress. Antioxid Redox Signal 2016;25:657–684
5. Jha JC, Gray SP, Barit D, et al. Genetic targeting or pharmacologic inhibition of NADPH oxidase Nox4 provides renoprotection in long-term diabetic nephropathy. J Am Soc Nephrol 2014;25:1237–1254
6. Gorin Y, Block K, Hernandez J, et al. Nox4 NAD(P)H oxidase mediates hypertrophy and fibronectin expression in the diabetic kidney. J Biol Chem 2005;280:39616–39626
7. Jha JC, Thallas-Bonke V, Banal C, et al. Podocyte-specific Nox4 deletion affords renoprotection in a mouse model of diabetic nephropathy. Diabetologia 2016;59:379–389
8. Sedeek M, Gutsol A, Montezano AC, et al. Renoprotective effects of a novel Nox1/4 inhibitor in a mouse model of type 2 diabetes. Clin Sci (Lond) 2013;124:191–202
9. Thallas-Bonke V, Jha JC, Gray SP, et al. Nox-4 deletion reduces oxidative stress and injury by PKC-α-associated mechanisms in diabetic nephropathy. Physiol Rep 2014;2:e12192.
10. Di Marco E, Gray SP, Kennedy K, et al. NOX4-derived reactive oxygen species limit fibrosis and inhibit proliferation of vascular smooth muscle cells in diabetic atherosclerosis. Free Radic Biol Med 2016;97:556–567
11. Gray SP, Di Marco E, Kennedy K, et al. Reactive oxygen species can provide atheroprotection via NOX4-dependent inhibition of inflammation and vascular remodeling. Arterioscler Thromb Vasc Biol 2016;36:295–307
12. Schürmann C, Rezende F, Kruse C, et al. The NADPH oxidase Nox4 has anti-atherosclerotic functions. Eur Heart J 2015;36:3447–3456
13. Aoyama T, Paik YH, Watanabe S, et al. Nicotinamide adenine dinucleotide phosphate oxidase in experimental liver fibrosis: GKT137831 as a novel potential therapeutic agent. Hepatology 2012;56:2316–2327
14. Gray SP, Jha JC, Kennedy K, et al. Combined NOX1/4 inhibition with GKT137831 in mice provides dose-dependent reno- and atheroprotection even in established micro- and macrovascular disease. Diabetologia 2017;60:927–937
15. Teixeira G, Szyndralewiez C, Molango S, et al. Therapeutic potential of NADPH oxidase 1/4 inhibitors. Br J Pharmacol 2017;174:1647–1669
16. Holterman CE, Boisvert NC, Thibodeau JF, et al. Podocyte NADPH oxidase 5 promotes renal inflammation regulated by the Toll-like receptor pathway. Antioxid Redox Signal 2019;30:1817–1830.
17. Jha JC, Banal C, Okabe J, et al. NADPH oxidase Nox5 accelerates renal injury in diabetic nephropathy. Diabetes 2017;66:2691–2703
18. Jha JC, Dai A, Holterman CE, et al. Endothelial or vascular smooth muscle cell-specific expression of human NOX5 exacerbates renal inflammation, fibrosis and albuminuria in the Akita mouse. Diabetologia 2019;62:1712–1726
19. Deliyanti D, Alrashdi SF, Touyz RM, et al. Nox (NADPH oxidase) 1, Nox4, and Nox5 promote vascular permeability and neovascularization in retinopathy. Hypertension 2020;75:1091–1101
20. Guzik TJ, Chen W, Gongora MC, et al. Calcium-dependent NOX5 nicotinamide adenine dinucleotide phosphate oxidase contributes to vascular oxidative stress in human coronary artery disease. J Am Coll Cardiol 2008;52:1803–1809
21. Touyz RM, Anagnostopoulou A, Camargo LL, Rios FJ, Montezano AC. Vascular biology of superoxide-generating NADPH oxidase 5-implications in hypertension and cardiovascular disease. Antioxid Redox Signal 2019;30:1027–1040
22. Carmo LSD, Berk BC, Harrison DG. NOX5 as a therapeutic target in cerebral ischemic injury. J Clin Invest 2019;129:1530–1532
23. Kleinschnitz C, Grund H, Wingler K, et al. Post-stroke inhibition of induced NADPH oxidase type 4 prevents oxidative stress and neurodegeneration. PLoS Biol 2010;8:e1000479
24. Sato S, Sasaki Y, Adachi A, Ghazizadeh M. Validation of glomerular basement membrane thickness changes with aging in minimal change disease. Pathobiology 2010;77:315–319
25. Lim AK, Tesch GH. Inflammation in diabetic nephropathy. Mediators Inflamm 2012;2012:146154
26. Meier M, Park JK, Overheu D, et al. Deletion of protein kinase C-β isoform in vivo reduces renal hypertrophy but not albuminuria in the streptozotocin-induced diabetic mouse model. Diabetes 2007;56:346–354
27. Urner S, Ho F, Jha JC, Ziegler D, Jandeleit-Dahm K. NADPH oxidase inhibition: preclinical and clinical studies in diabetic complications. Antioxid Redox Signal 2020;33:415–434
28. Fulton DJ. Nox5 and the regulation of cellular function. Antioxid Redox Signal 2009;11:2443–2452
29. Chow FY, Nikolic-Paterson DJ, Ozols E, Atkins RC, Rollin BJ, Tesch GH. Monocyte chemoattractant protein-1 promotes the development of diabetic renal injury in streptozotocin-treated mice. Kidney Int 2006;69:73–80
30. Lin M, Yiu WH, Wu HJ, et al. Toll-like receptor 4 promotes tubular inflammation in diabetic nephropathy. J Am Soc Nephrol 2012;23:86–102
31. Mudaliar H, Pollock C, Panchapakesan U. Role of Toll-like receptors in diabetic nephropathy. Clin Sci (Lond) 2014;126:685–694
32. Cha JJ, Hyun YY, Lee MH, et al. Renal protective effects of Toll-like receptor 4 signaling blockade in type 2 diabetic mice. Endocrinology 2013;154:2144–2155
33. Pushpakumar S, Ren L, Kundu S, Gamon A, Tyagi SC, Sen U. Toll-like receptor 4 deficiency reduces oxidative stress and macrophage mediated inflammation in hypertensive kidney. Sci Rep 2017;7:6349
34. Ho LC, Sung JM, Shen YT, et al. Egr-1 deficiency protects from renal inflammation and fibrosis. J Mol Med (Berl) 2016;94:933–942
35. Hu F, Xue M, Li Y, et al. Early growth response 1 (Egr1) is a transcriptional activator of NOX4 in oxidative stress of diabetic kidney disease. J Diabetes Res 2018;2018:3405695
36. Hu F, Xue R, Wei X, et al. Egr1 knockdown combined with an ACE inhibitor ameliorates diabetic kidney disease in mice: blockade of compensatory renin increase. Diabetes Metab Syndr Obes 2020;13:1005–1013
37. Ha H, Yu MR, Choi YJ, Lee HB. Activation of protein kinase c-δ and c-ε by oxidative stress in early diabetic rat kidney. Am J Kidney Dis 2001;38(Suppl. 1):S204–S207
38. Ma L, Wu F, Shao Q, Chen G, Xu L, Lu F. Baicalin alleviates oxidative stress and inflammation in diabetic nephropathy via Nrf2 and MAPK signaling pathway. Drug Des Devel Ther 2021;15:3207–3221
39. Advani A, Gilbert RE, Thai K, et al. Expression, localization, and function of the thioredoxin system in diabetic nephropathy. J Am Soc Nephrol 2009;20:730–741
40. Saxena G, Chen J, Shalev A. Intracellular shuttling and mitochondrial function of thioredoxin-interacting protein. J Biol Chem 2010;285:3997–4005
41. Shah A, Xia L, Masson EA, et al. Thioredoxin-interacting protein deficiency protects against diabetic nephropathy. J Am Soc Nephrol 2015;26:2963–2977
42. Thomasova D, Anders HJ. Cell cycle control in the kidney. Nephrol Dial Transplant 2015;30:1622–1630
43. McLennan SV, Wang XY, Moreno V, Yue DK, Twigg SM. Connective tissue growth factor mediates high glucose effects on matrix degradation through tissue inhibitor of matrix metalloproteinase type 1: implications for diabetic nephropathy. Endocrinology 2004;145:5646–5655
44. van Nieuwenhoven FA, Jensen LJ, Flyvbjerg A, Goldschmeding R. Imbalance of growth factor signalling in diabetic kidney disease: is connective tissue growth factor (CTGF, CCN2) the perfect intervention point? Nephrol Dial Transplant 2005;20:6–10
45. Burns WC, Twigg SM, Forbes JM, et al. Connective tissue growth factor plays an important role in advanced glycation end product-induced tubular

epithelial-to-mesenchymal transition: implications for diabetic renal disease. J Am Soc Nephrol 2006;17:2484–2494
46. Loeffler I, Wolf G. Epithelial-to-mesenchymal transition in diabetic nephropathy: fact or fiction? Cells 2015;4:631–652
47. Oldfield MD, Bach LA, Forbes JM, et al. Advanced glycation end products cause epithelial-myofibroblast transdifferentiation via the receptor for advanced glycation end products (RAGE). J Clin Invest 2001;108:1853–1863
48. Cooper ME, Vranes D, Youssef S, et al. Increased renal expression of vascular endothelial growth factor (VEGF) and its receptor VEGFR-2 in experimental diabetes. Diabetes 1999;48:2229–2239
49. Eremina V, Jefferson JA, Kowalewska J, et al. VEGF inhibition and renal thrombotic microangiopathy. N Engl J Med 2008;358:1129–1136
50. Menne J, Park JK, Boehne M, et al. Diminished loss of proteoglycans and lack of albuminuria in protein kinase C-α-deficient diabetic mice. Diabetes 2004;53:2101–2109
51. Menne J, Shushakova N, Bartels J, et al. Dual inhibition of classical protein kinase C-α and protein kinase C-β isoforms protects against experimental murine diabetic nephropathy. Diabetes 2013;62:1167–1174
52. Fioretto P, Mauer M. Histopathology of diabetic nephropathy. Semin Nephrol 2007;27:195–207